Supplementary Figure S1

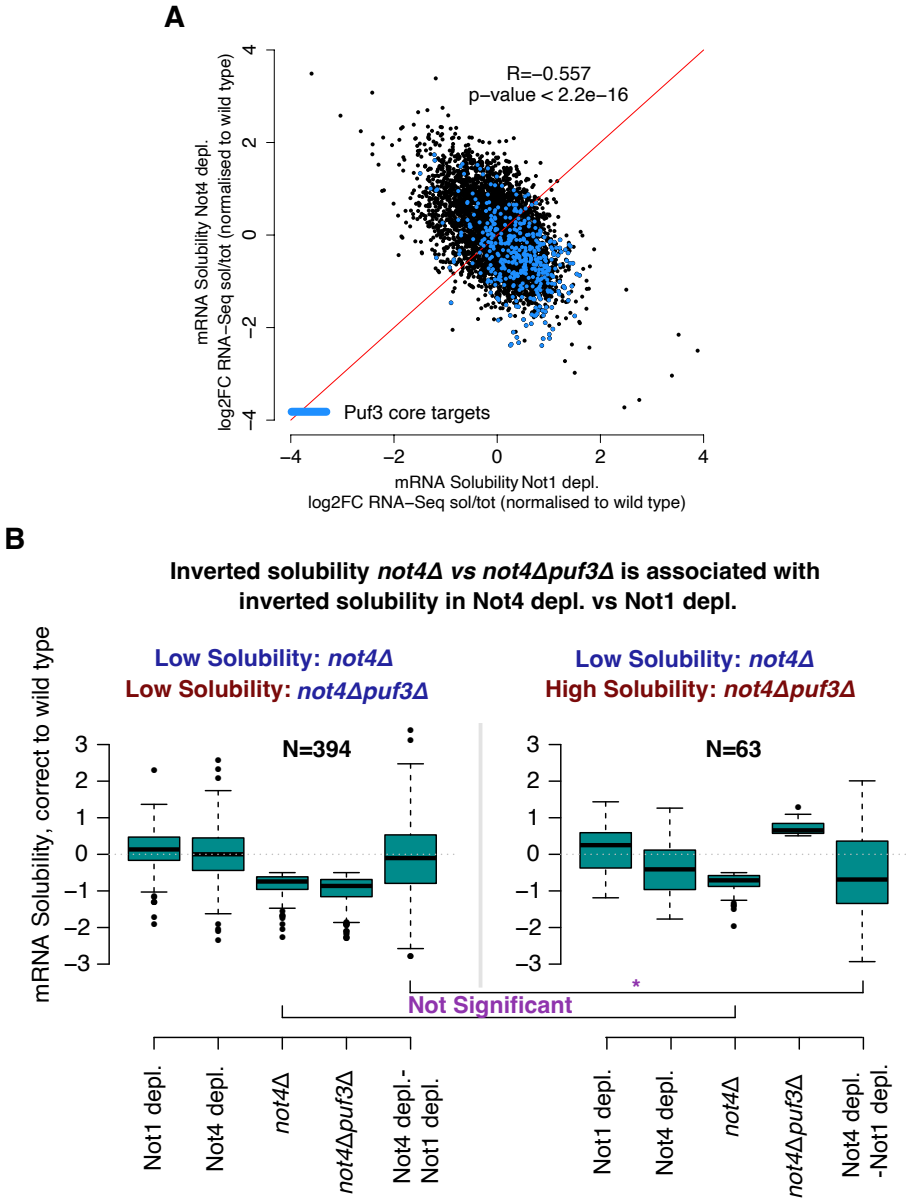

Supplementary Figure S1. Puf3 targets are enriched within mRNAs less soluble upon Not4 depletion but more soluble upon Not1 depletion. Related to **Figure 1. A.** Scatterplot showing inverse changes in mRNA solubilities upon Not1 (x-axis) and Not4 (y-axis) depletion (17). Wild type is indicated by WT. Puf3 target mRNAs are indicated in blue**. B.** The 394 mRNAs that show decrease in solubility in *not4Δ* and *not4Δpuf3Δ* compared to wild type (log_2 fold change smaller than -0.5) are represented in the left panel whereas the 63 mRNAs that show a decrease in solubility in *not4Δ* compared to wild type (log_2 fold change smaller than -0.5) but an increase solubility in *not4Δpuf3Δ* (log_2 fold change greater than 0.5) are represented in the right panel. The change in solubility of each pool of mRNAs upon Not1 and Not4 depletion is represented in the first and second columns of each panel and the difference in change of solubility of each pool of mRNAs upon Not1 and Not4 depletion is shown in the far-right column of each panel. A Welch's t-test was used to perform the statistical analysis. This shows that the solubility of the 63 mRNAs is significantly inversely regulated upon Not1 and Not4 depletion compared to the 394 whose solubility is not differentially impacted upon Not1 and Not4 depletion.

Supplementary Figure S2

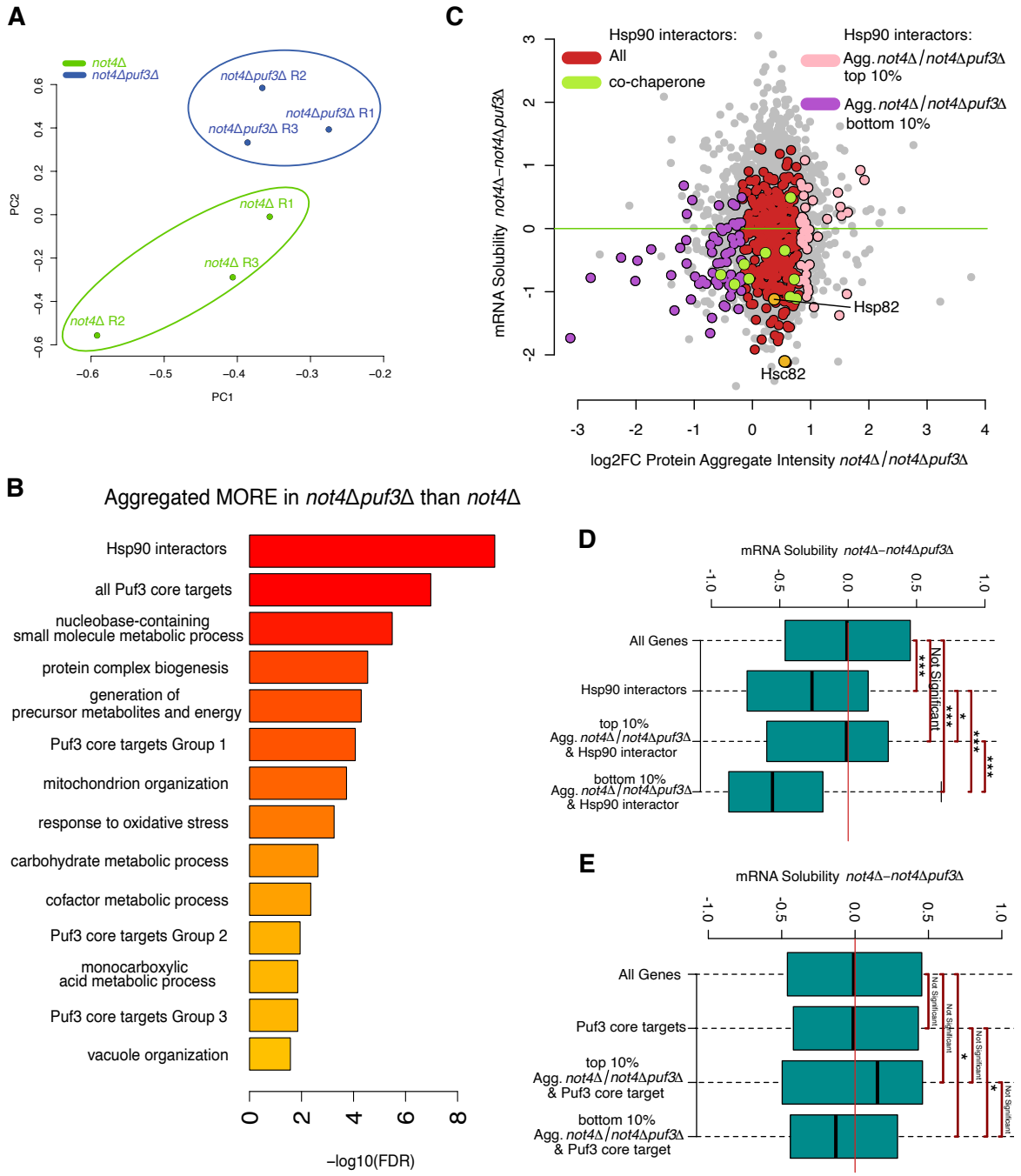

Supplementary Figure S2. Analysis by quantitative mass spectrometry of proteins in aggregates in *not4Δ* and *not4Δpuf3Δ*. Related to **Figure 2. A.** Pincipal Component Analysis (PCA) of the triplicate samples of *not4Δ* and *not4Δpuf3Δ* that were analyzed by quantitative mass spectrometry shows clustering of group samples. **B.** GO-term analysis of proteins that are more present in aggregates in the double mutant. **C.** Scatterplot indicating changes in protein aggregation intensity (x-axis) and solubility of encoding mRNA changes (y-axis) in the single versus the double mutant. The Hsc82 and Hsp82 (the Hsp90 chaperones) are indicated in orange. The Hsp90 interactors are highlighted in color, in pink are the interactors whose increase in aggregate intensity in the single mutant relative to the double falls in the top 10%, in purple those whose increase in aggregate intensity in the single mutant relative to the double falls in the bottom 10% and in red all other interactors. Hsp90 co-chaperones are highlighted in green. In grey are all other proteins. **D.** Box plot analysis comparing mRNA solubility changes compared to the wild type of the *not4Δ* single mutant relative to the *not4Δpuf3Δ* double mutant (y-axis) for different sets of mRNAs. The first upper line shows all transcripts. The second line shows transcripts encoding the Hsp90 interactors. The third and fourth lines show transcripts encoding the Hsp90 interactors with aggregation rate ratios of encoded proteins from single to double mutant that fall in the top (third line) and bottom (fourth line) 10%, respectively. A two-sided Welch's t-test was used to perform all pairwise comparisons. **E.** Box plot analysis comparing mRNA solubility changes compared to the wild type of the *not4Δ* single mutant relative to the *not4Δpuf3Δ* double mutant (y-axis) for different sets of mRNAs. The first upper line shows all transcripts. The second line shows all Puf3 core targets. The third and fourth lines show Puf3 targets with aggregation rate ratios of encoded proteins from single to double mutant that fall in the top (third line) and bottom (fourth line) 10%, respectively. A two-sided Welch's t-test was used to perform all pairwise comparisons.

Supplementary Figure S3

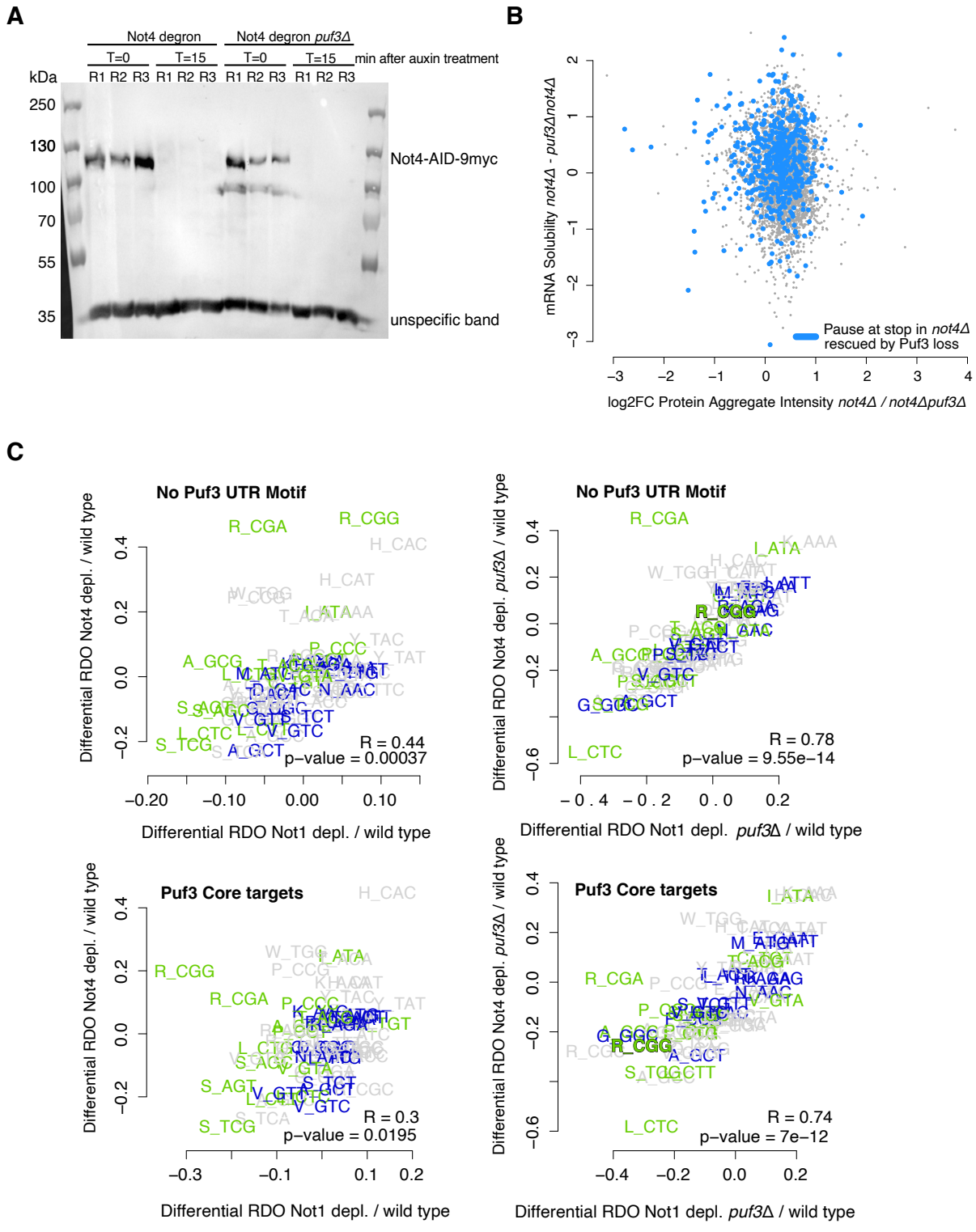

Supplementary Figure S3. Features of Ribo-Seq upon Not1 and Not4 depletion in presence or absence of Puf3. Related to **Figure 3**. **A.** Depletion of Not4-AID-9myc was assessed by western blot analysis with antibodies to myc, before (t=0) or after (t=15) addition of auxin for 15 min, for the triplicate samples R1, R2 and R3, in the Not4 degron strain, with or without an additional deletion of Puf3, as indicated. Molecular weight markers (in kDa) are indicated on the left. **B.** Scatter plot comparing changes in mRNA solubility (y-axis) and protein aggregation (x-axis) in *not4Δ* versus *not4Δpuf3Δ* for mRNAs that show increased pausing at stop upon Not4 depletion rescued by *puf3Δ* (in blue), and all other mRNAs in grey. Solubility is a $\log_2$ fold change of soluble/total expression for each strain, so the values are subtracted between strains. **C.** Scatterplot analyses comparing codon-specific changes in A-site RDOs, upon Not1 and Not4 depletion; in cells expressing or lacking Puf3 for Puf3 target mRNAs or mRNAs that are not targets of Puf3 (no Puf3 UTR Motif) as indicated.

Supplementary Figure S4

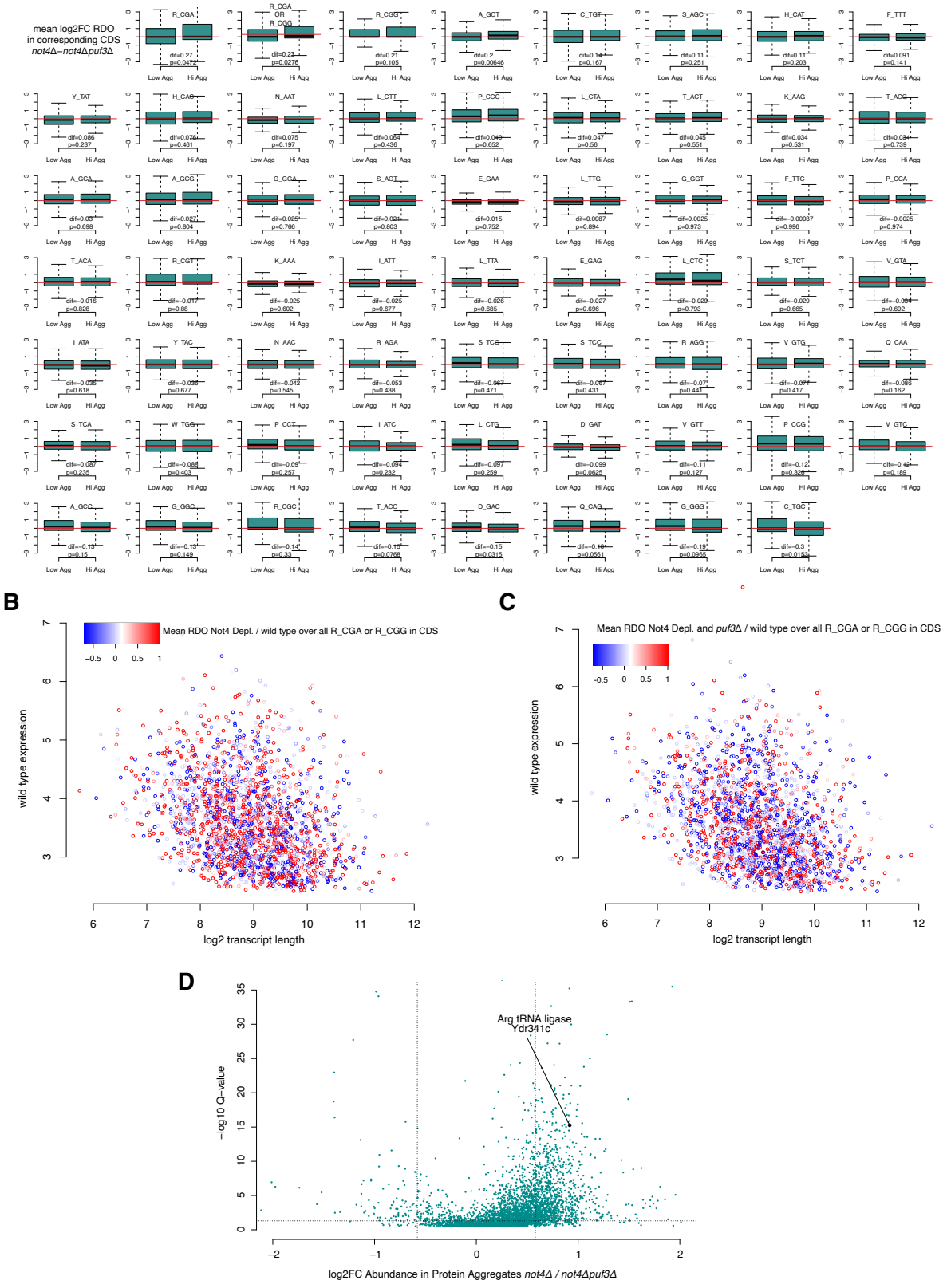

Supplementary Figure S4

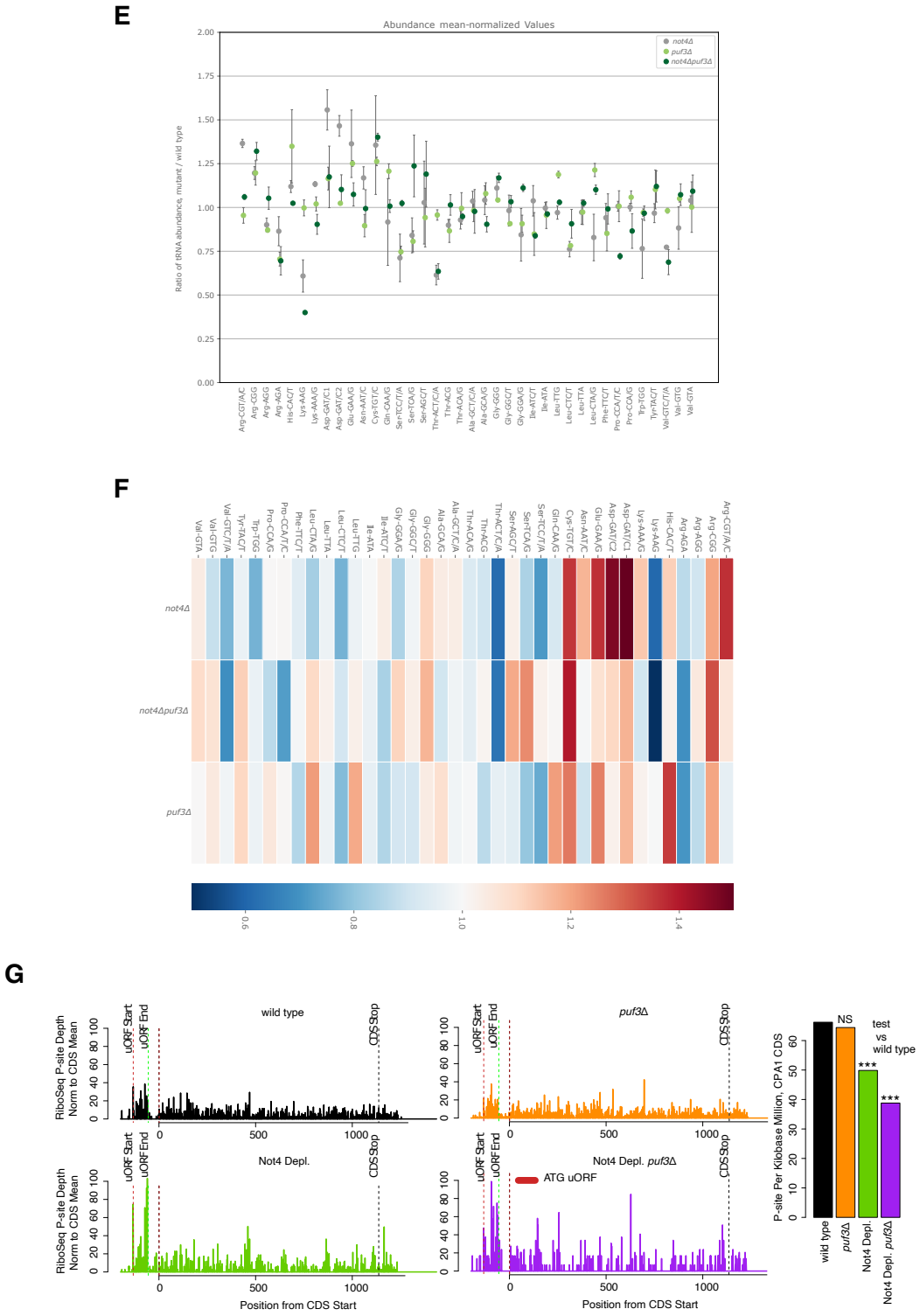

Supplementary Figure S4. For mRNAs showing loss of aggregation of encoded protein compared to those that do not, dwelling at rare arginine codons when comparing *not4Δ* to *not4Δpuf3Δ* is the most reduced. Related to **Figure 4. A**. Changes in codon-specific A-site RDOs for the 300 mRNAs whose encoded proteins aggregate the least in the *not4Δ* single mutant compared to the double *not4Δpuf3Δ* (designated as "Low Agg") compared to the 300 mRNAs whose encoded proteins show the highest aggregation in the single compared to the double mutant ("Hi Agg") were evaluated. The results are shown by box plots for each codon that are ordered from the greatest difference (top left) to the lowest (bottom right). **B** and **C**. Scatterplots of all mRNAs according to the length (x-axis) and their mean expression level in wild type cells (WT) assessed from the Ribo-Seq (y-axis). mRNAs were color coded according to the changes in average A-site RDOs at rare arginine codons in the whole CDS in the mutant compared to the wild type. **B.** the mutant is Not4 depletion and **C.** the mutant is Not4 depletion and *puf3Δ*. **D**. The arginyl-tRNA synthetase is labelled in the volcano plot from **Figure 2C** to show that it is more present in protein aggregates from *not4Δ* than from *puf3Δnot4Δ.* **E**. tRNA levels measured in *puf3Δ* and *puf3Δnot4Δ*, compared to wild type by tRNA-microarrays are presented as relative expression to wild type. For comparison, the data in *not4Δ* compared to wild type measured earlier (19) are included. **F.** tRNA charging using tRNA microarrays measured in *puf3Δ* and *puf3Δnot4Δ* compared to wild type. The measurements in wild type and *not4Δ* as determined earlier (19) are included for comparison. The color key indicates the percentage of charged tRNAs over the total amount of each isoacceptor. The microarrays were performed in duplicates and represented as mean values. Confidence intervals between both replicates is 97% for *puf3Δ,* 99% for *puf3Δnot4Δ,* 95% for *not4Δ*, and 98% for wild type, respectively. In **E-F**, tRNA probes are depicted with their cognate codon and the corresponding amino acid. **G**. Ribo-Seq P-site depths at the *CPA1* locus, both upstream ORF and CDS sequences, in wild type (WT), upon Not4 depletion, in *puf3Δ* and upon Not4 depletion and *puf3Δ* (left 4 panels) and on the right is a barplot of P-sites per kilobase million on the CDS for all these strains with significance test of expression change versus wild type (WT) for all non-wild type strains. The P-site depths at each position on *CPA1* mRNA in the Not4 depletion strain and in the Not4 depletion strain deleted for Puf3 were normalized to the CDS mean and both showed high values in the uORF, relative to the main CDS.

Supplementary Figure S5

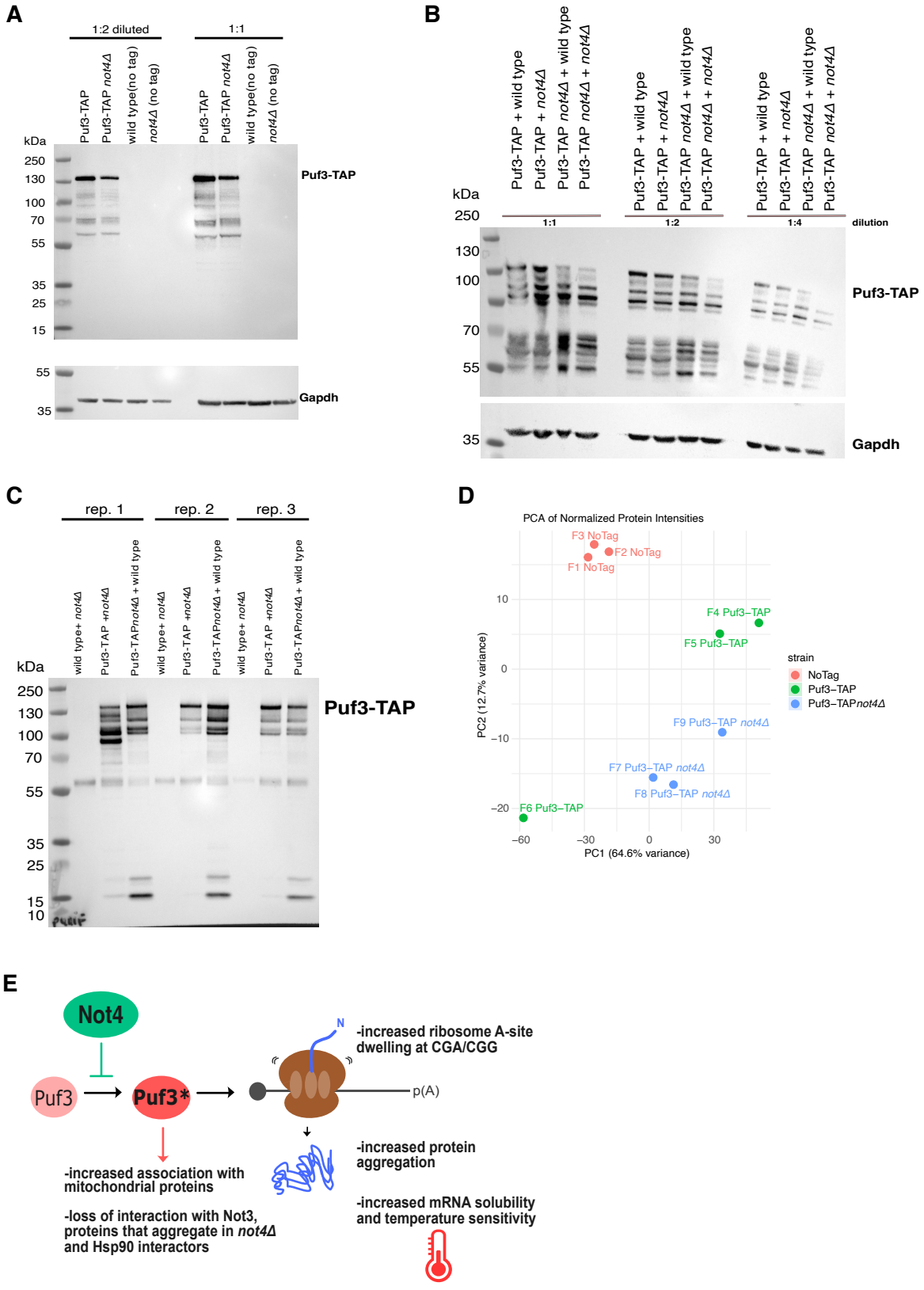

Supplementary Figure S5. Quality controls for the identification of differential interactomes of Puf3 from wild type and *not4Δ* cells. Related to **Figure 5**. **A.** Total protein using post-alkaline lysis from wild type and *not4Δ* cells expressing Puf3-TAP were analyzed by western blotting with antibodies to Protein A, revealing slightly reduced levels of Puf3-TAP in the mutant. Antibodies against Gapdh were used as loading control. **B**. For the Puf3 integrity test, prior to centrifugation cells were mixed as indicated in the legend above the blot, and the cell pellet was collected for lysis with glass beads and protein extraction. The lysates were analyzed by western blotting using antibodies to Protein A and to Gapdh for a loading control. The full-length Puf3-TAP seems to migrate at approximately 130 kDa and is indicated to the right of the blot. Faster migrating bands could correspond to degradation products (more abundant in lysates than in total extracts obtained by post-alkaline lysis, compare this panel to panel **A**). **C.** Western blot analysis with antibodies to Protein A to follow the triplicate purifications of Puf3-TAP for mass spectrometry analysis. **D.** PCA, based on normalized protein levels reveals clustering of group samples except replicate 2 for Puf3-TAP (F6 Puf3-TAP). **E.** Model for the functional interaction between Not4 and Puf3. In absence of Not4, Puf3 is modified (for instance post-translationally and/or in its' interaction partners including Not3 and mitochondrial proteins, and/or in its ability to form condensates) and this leads to changes in translation elongation dynamics in particular at rare arginine codons and to protein aggregation and temperature sensitivity.